Catalysis Communications 69 (2015) 217–222

Contents lists available at ScienceDirect

Catalysis Communications

journal homepage: www.elsevier.com/locate/catcom

Hydrodesulfurization of dibenzothiophene over PtMo/MCM-48 catalysts

Marcelo J.B. Souza [a,*], Anne M. Garrido Pedrosa [b], Juan A. Cecilia [c], Antonio M. Gil-Mora [c], Enrique Rodríguez-Castellón [c]

[a] Federal University of Sergipe, Departament of Chemical Engineering (DEQ), Cidade Universitária Professor José Aloísio de Campos, Avenida Marechal Rondon, S/N, Jardim Rosa Elze, São Cristóvão/SE 49100-000, Brazil

[b] Federal University of Sergipe, Departament of Chemistry (DQJ), Cidade Universitária Professor José Aloísio de Campos, Avenida Marechal Rondon, S/N, Jardim Rosa Elze, São Cristóvão/SE 49100-000, Brazil

[c] University of Málaga, Department of Inorganic Chemistry, Crystallography and Mineralogy, Faculty of Sciences, 29071 Málaga, Spain

ARTICLE INFO

Article history:
Received 18 February 2015
Received in revised form 1 July 2015
Accepted 3 July 2015
Available online xxxx

Keywords:
Hydrodesulfurization
MCM-48
XPS

ABSTRACT

Catalysts of platinum and molybdenum supported on MCM-48 materials were synthesized and characterized by XRD, XPS and N_2 adsorption–desorption. Catalytic activity was evaluated in the model reaction of hydrodesulfurization of dibenzothiophene. Catalytic results showed high catalytic performance of ca. 95% for PtMo/MCM-48 catalyst with the formation of biphenyl (BP) as the main product, typical from direct hydrodesulfurization (DDS) pathway and ciclohexylbenzene (CHB) in a minor proportion from the hydrogenation prior to the desulfurization pathway.

1. Introduction

In the last decades, environmental legislations are aimed to minimize the pollutant gas emissions to the atmosphere. In this sense, the sulfur removal from petroleum feedstock has been an important issue of global concern due to the sulfur in fuels acts as pollutant [1–5]. The use of noble metals as active phases or as promoters has attained a high interest due to the good performance in hydrotreating (HDT) and hydrogenation (HYD) reactions [6,7]. Previous works in the literature studied systems with PtMo supported on Al_2O_3 [8] and PtMo supported the mesoporous silica–alumina (MSA) [9] with disordered pore structure, respectively. In this work, systems with PtMo supported on siliceous MCM-48 nanostructured material were studied. MCM-48 materials present pores systems of three-dimensional with diameters that can vary from 15 to 100 Å [10–13]. This fact suggests that this framework is potentially more advantageous for catalytic and adsorptive applications compared with one-dimensional pores catalysts, due to the diffusion of the reagents and products through the pores is favored, being less prone to blockages [14].

MCM-48 has been used as support using transition metals sulfides as active phase and catalytic systems have shown to be an important alternative for the development of catalysts capable of acting on several industrial processes that need reactivity on hydrogenolysis, hydrogenation reactions and on the reduction of sulfur compounds present in fossil fuels via HDS reactions [15,16]. The present work aims to develop of catalysts containing platinum and molybdenum species supported on MCM-48 for the hydrodesulfurization (HDS) of dibenzothiophene (DBT) model reaction. XPS analysis [17–19] was performed to evaluate the active phases present on the surface of the catalysts, before and after the catalytic reaction in order to know whether changes occurred in the phases present on the surface. For the catalyst containing amorphous phases, the XPS is an essential technique to identify the active species on the surface.

2. Experimental

MCM-48 material was synthesized by hydrothermal method using as reactants tetraethoxysilane (TEOS, Aldrich, 98.0%), sodium hydroxide (Vetec, 98.0%), hexadecyltrimethylammonium bromide (Vetec, 98.0%) and distilled water. MCM-48 synthesis was made using a procedure based on that developed by Doyle et al. [20] and other procedures [21]. The molar composition used to prepare the synthesis gel was: $1.0SiO_2$: $0.25Na_2O$: 0.55CTMABr: $100.4H_2O$ [21].

The MCM-48 materials containing platinum, molybdenum and platinun + molybdenum species were prepared by the incipient wetness co-impregnation using ammonium tetrachloroplatinate(II) (Sigma-Aldrich, 99.0%) and ammonium molybdate tetrahydrate (Fluka, 99.0%), respectively. The solids were dried at 80 °C by 24 h and calcined at 450 °C for 2 h with a heating rate of 5 °C min^{-1}. The composition of the prepared samples was: 2.0% of Pt on MCM-48 (Pt/MCM-48), 2.0% of Mo on MCM-48 (Mo/MCM-48) and 1.0% of Pt and 1.0% of Mo on MCM-48 (PtMo/MCM-48).

* Corresponding author at: Universidade Federal de Sergipe, Departamento de Engenharia Química, 49100-000 São Cristóvão/SE, Brazil.
E-mail address: marcelojbs@ufs.br (M.J.B. Souza).

http://dx.doi.org/10.1016/j.catcom.2015.07.004
1566-7367/

XRD measurements were carried out with a Rigaku (MiniFlex II) X-ray equipment using CuKα radiation in 2θ angle of 1.5° to 10° and until 60° with step of 0.01°. Nitrogen adsorption–desorption analyses were performed at −196 °C by using a Quantachrome equipment (NOVA 1200e). Before sorption measurements the samples were degassed at 250 °C for 4 h. The specific surface area (SSA) was calculated using the Brunauer–Emmett–Teller (BET) method for relative pressure (P/P_0) ranged between 0.05 and 0.20. Pore volume (Vp) were determined by nitrogen adsorption at a relative pressure of 0.99 and pore size distributions from the branch isotherms adsorption by Barrett–Joyner–Halenda (BJH) method were also taken into account.

X-ray photoelectron spectra were collected using a Physical Electronics PHI 5700 spectrometer with non-monochromatic Mg Kα radiation (300 W, 15 kV and 1486.6 eV) with a multi-channel detector. Spectra of samples were recorded in the constant pass energy mode at 29.35 eV, using a 720 μm diameter analysis area. Charge referencing was measured against adventitious carbon (C 1 s at 284.8 eV). A PHI ACCESS ESCA-V6.0 F software package was used for acquisition and data analysis. The spectrometer energy scale was calibrated using Cu $2p_{3/2}$, Ag $3d_{5/2}$ and Au $4f_{7/2}$ photoelectron lines at 932.7, 368.3 and 84.0 eV, respectively. Surface atomic concentrations were determined taking into account the corresponding area sensitivity factor for the different measured spectral regions. The Mo 3d spectra were fitted with a doublet Mo $3d_{5/2}$-Mo $3d_{3/2}$ separation of 3.2 eV and an area ratio 3:2 and a FWHM of 3.3 eV, while the Pt 4f spectra were fitted with Pt $4f_{7/2}$-Pt $4f_{5/2}$ separation of 3.3 eV and an area ratio 4:3 and a FWHM of 2.0 eV.

HDS of DBT was performed in a high-pressure fixed-bed continuous flow stainless steel catalytic reactor (PID Instruments) at 3.0 MPa of H_2 with flow rate of 100 ml min^{-1} and organic feed of 0.3 ml min^{-1}. The organic feed consisted of a solution of 1% wt of DBT (Aldrich, 99%) in cis-, trans-decahydronaphthalene (Sigma-Aldrich, 98%). For the activity tests, 0.5 g of catalyst was used (particle size 0.85–1.00 mm) and was diluted with quartz sand to 3 cm^3. Prior to the activity test, the catalysts were sulfided in situ at atmospheric pressure with a N_2/H_2S (90/10%) flow of 60 ml min^{-1} by heating from rt. to 500 °C (2 h) at a heating rate of 10 °C min^{-1}. Catalytic activities were measured at different temperatures (250–375 °C) and samples were collected and analyzed by gas chromatography (Shimadzu GC-14B) equipped with a flame ionization detector and a capillary column (TBR-14).

3. Results

XRD pattern for MCM-48 used as support is shown in Fig. 1a. The diffractogram displays reflection lines in the range of 2θ = 1.5–5.5°. The more intense diffraction line located at 2θ = 2.60° is attributed to the plane (211) while the other seven peaks located between 2.83° and 5.11° have been designed to reflections (220), (321), (400), (420), (332), (422) and (431), respectively, which are indexed for *Ia3d* space group and are in accordance with various XRD patterns reported in the literature of the cubic phase MCM-48 [20,21]. After the impregnation with platinum and molybdenum species, XRD data reveal a shift of the main diffraction line (211) and in the mesoporous parameters (a_o) of the MCM-48 cubic structure (Fig. 1b and c, and Table 1), due to the incorporation both platinum and molybdenum species in the pores of the material [22]. The XRD of Pt/MCM-48 and PtMo/MCM-48 showed well-defined diffraction lines located at 2θ = 39.76° (plane (111)) and 46.24° (plane (200)), corresponding to cubic metallic platinum phase (ICDD card No 04–0802) (Fig. 2a and b). Fig. 2b shows the XRD patterns of the catalysts after sulfidation and shows that the intensity of the diffraction lines attributed to Pt species decreases, in the case of Pt/MCM-48 and PtMo/MCM-48 catalysts. The Pt metal particle sizes were calculated by Scherrer equation: Pt/MCM-48 (oxide) = 24.6 nm; Pt/MCM-48 (sulfided) = 18.2 nm; PtMo/MCM-48 (oxide) = 21.4 nm and PtMo/MCM-48 (sulfided) = 16.1 nm.

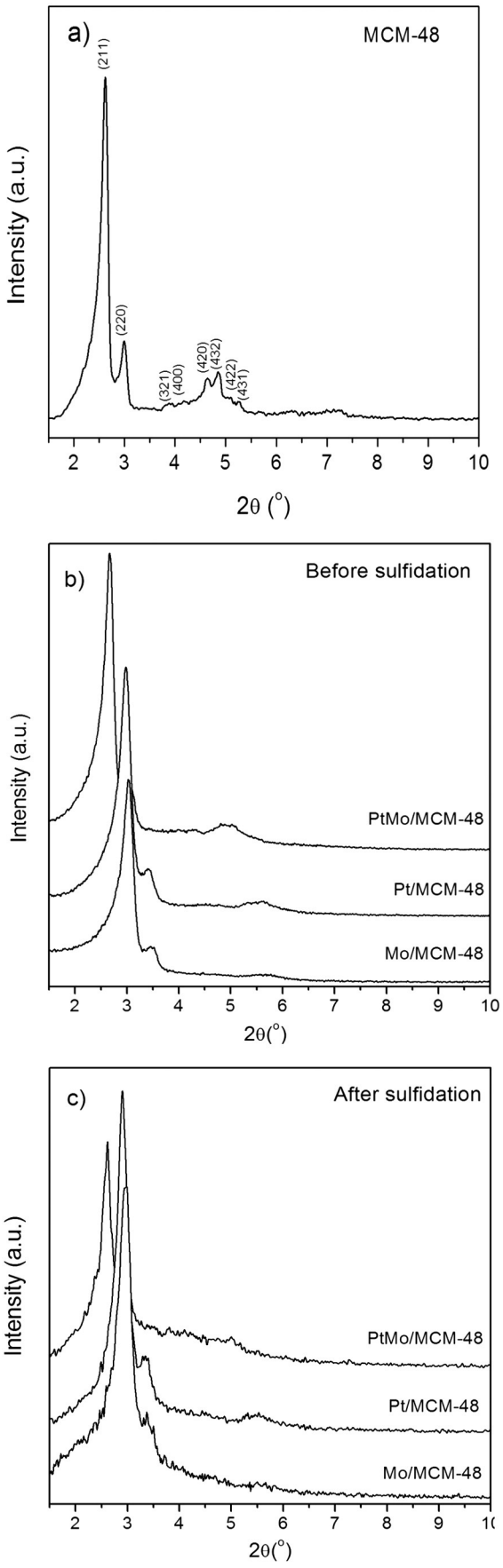

Fig. 1. XRD of the materials at low angle: a) Support MCM-48, b) catalysts before sulfidation and b) catalysts after sulfidation.

Table 1
Textural properties of the catalysts.

Samples	a_o (nm)	SSA ($m^2\ g^{-1}$)	W_t (nm)	D_p (nm)	V_p ($cm^3\ g^{-1}$)
Suport	8.42	1325	0.87	3.70	0.19
PtMo/MCM-48[b]	8.11	989	0.77	3.71	0.16
Pt/MCM-48[b]	7.29	1053	0.50	3.71	0.17
Mo/MCM-48[b]	7.15	1075	0.56	3.50	0.18
PtMo/MCM-48[a]	8.29	546	1.32	2.72	0.17
Pt/MCM-48[a]	7.43	735	0.52	3.76	0.14
Mo/MCM-48[a]	7.28	534	1.20	2.30	0.12

Where: a = after sulfidation and b = before sulfidation, a_o = mesoporous parameter, SSA = specific surface area; W_t = silica wall tickness; D_p = pore diameter and V_p = pore volume.

The nitrogen adsorption–desorption isotherms for the M/MCM-48 (where M = Pt, Mo or PtMo) before and after sulfidation are shown in Fig. 3. The M/MCM-48 catalysts display a type IV isotherms in the IUPAC classification and a sharp inflection on the range of P/P_0 = 0.15 − 0.3, which takes places due the capillary condensation of nitrogen in the mesoporous [23]. The textural properties data of the catalysts are shown in Table 1. It is possible to observe that for all M/MCM-48 catalysts there was a decrease in the values of total area and pore volume in relation of the support. This decrease is more significant for sulfide samples, and in general can be related to significant blockage of the MCM-48 pores by platinum and–or molybdenum species and also due to partial loss of structural ordering of the mesoporous channels.

Table 2 shows the XPS analysis results of the PtMo/MCM-48 catalysts (in the oxide form, in the sulfided form and after HDS reaction), as the binding energies (eV) and the surface atomic concentration of core electrons.

In Fig. 4., Pt $4f_{7/2}$ core level spectra of Pt/MCM-48 and PtMo/MCM-48 catalysts as unsulfided, sulfided and after reaction show two contributions: a main contribution located about 71.5 eV, which is attributed to metallic platinum and a second contribution of lesser extend centered about 73.0 eV assigned to a small amount of Pt(II) in the form of PtO [24,25]. After the sulfidation step, both contributions remain unaltered for Pt/MCM-48 and PtMo/MCM-48 catalysts. Comparing the data presented in Table 2 with the data obtained by Dembowski and collaborators [26] it was not observed the formation of PtS or PtS_2 (Pt $4f_{7/2}$ = 72.55 and 74.16 eV, respectively) in the sulfided catalysts (S) and too in the after reaction catalysts (SPR). This fact suggests that platinum base catalysts present a high sulfur resistance which could favor the stability of the active phase during the catalytic test [8,26,27]. This can be correlated as a result of the differential interaction of platinum species formed with the support which has been attributed to an electronic deficiency of the metal, resulting of interaction with the support. Analysis of S $2p_{3/2}$ core level spectrum of PtMo/MCM-48 shows an unique contribution located at 162.3 eV which has been attributed to sulfide species.

In the case of containing molybdenum oxide precursor samples (Mo/MCM-48 and PtMo/MCM-48), Fig. 5 shows Mo $3d_{5/2}$ core level spectra XPS data of both catalytic precursor show an unique contribution located between 231.6 and 232.0 eV assigned to Mo^{6+} species in the form of MoO_3 [15].

When the samples are sulfided, both catalysts present two contribution: the main contribution, located about 228 eV, has been attributed to Mo^{4+} species in the form of MoS_2 and a minor contribution between 231.2 and 231.9 eV is ascribed to Mo^{6+} species in the form of unsulfided species and/or oxysulfide species. In the same way, S $2p_{3/2}$ core level spectra present the typical contribution ascribed to sulfide species, about 162 eV, corroborating the deep sulfidation of molybdenum species for the formation of MoS_2 species [15].

Table 3 shows the data of conversion of DBT over Pt/MCM-48, Mo/MCM-48 and PtMo/MCM-48 catalysts. In order to evaluate the stability of the catalysts as function of the time on stream [19], a

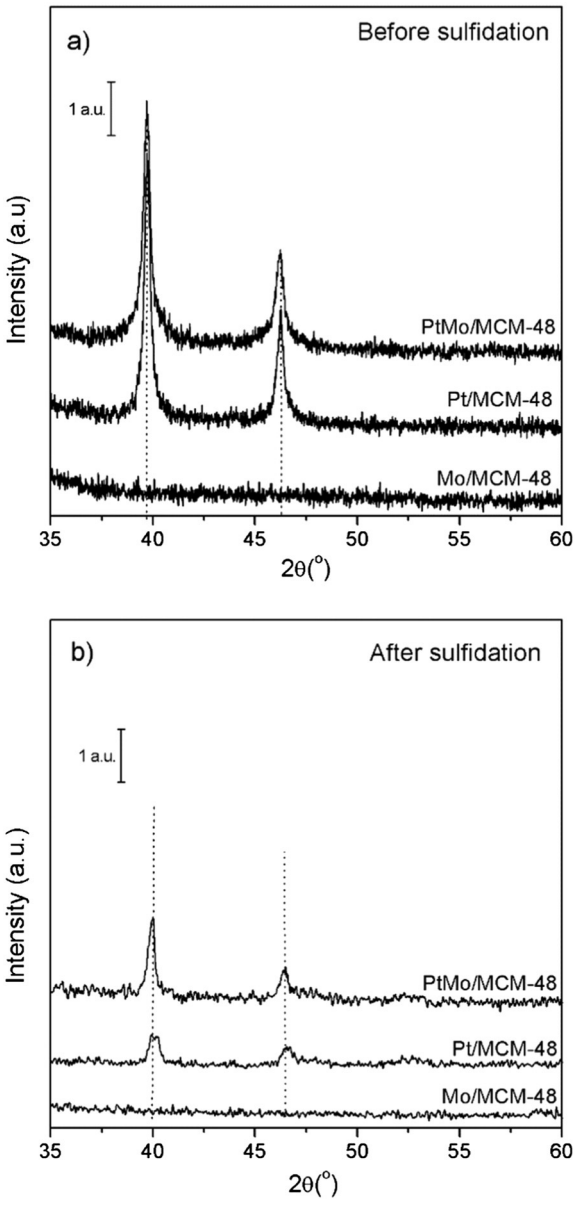

Fig. 2. XRD of the catalysts at high angle: a) before sulfidation and b) after sulfidation.

set of catalytic tests were performed at 350 °C during 8 h on stream (Table 4). With the increasing temperature occurred an increase in the DBT conversion and the yield also BP > CHB. These results possibly indicate that at high temperatures may have been promoted BP via direct hydrogenation of DBT, while production of CHB was observed in lesser amounts via the THDBT intermediary. BP product was obtained in larger quantities in all cases, reaching yields of 68.0, 17.8 and 0.8% for catalysts PtMo/MCM-48, Pt/MCM-48 and Mo/MCM-48, respectively after 8 h on stream. The HDS of DBT over sulfided CoMo/MCM-41 and $CoMo/Al_2O_3$ at 350 °C was previously reported and showed conversions of 58.5 and 30.7%, respectively [28].

The main reaction product was biphenyl (BP) in all catalysts, coming from the direct hydrogenolysis or direct desulfurization (DDS) pathway. Ciclohexylbenzene (CHB) also appears as by-product, although is formed in a lesser extend. This product is obtained from a hydrogenation of the rings prior the desulfurization (HYD) pathway through to tetrahydrodibenzothiophene (THDBT) intermediate. However, THDBT as intermediate possesses a very short life time in the catalytic cycle and thus it is expected does not appear in significant amounts in the products [29].

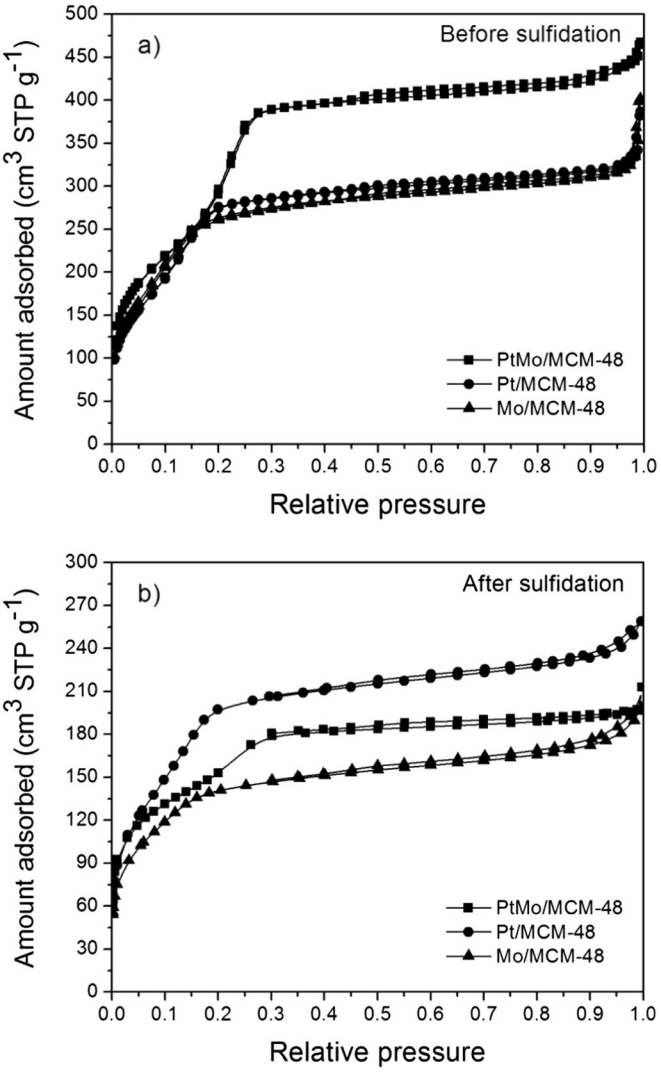

Fig. 3. Nitrogen adsorption isotherms of the catalysts: a) before sulfidation and b) after sulfidation.

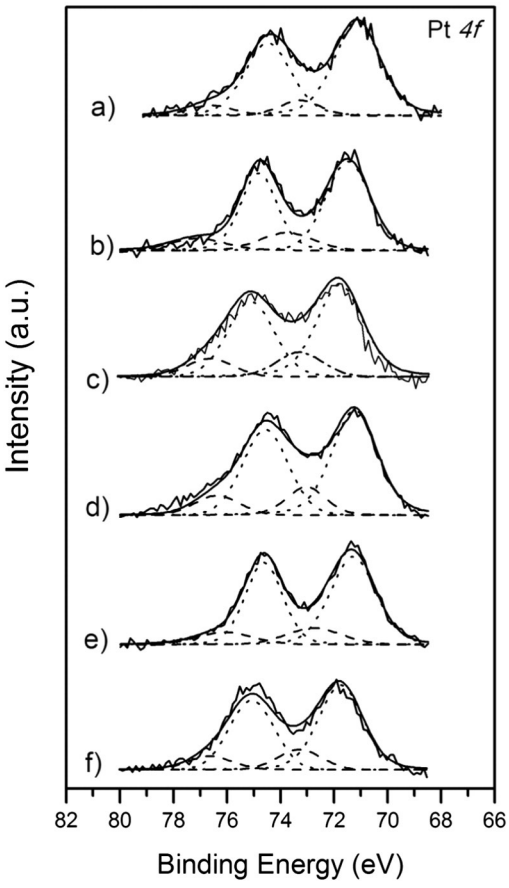

Fig. 4. Pt 4f core level spectra of PtMo/MCM-48 catalysts: (a) PtMo/MCM-48 (oxide), (b) PtMo/MCM-48 (sulfided), (c) PtMo/MCM-48 (after reaction), (d) Pt/MCM-48 (oxide), (e) Pt/MCM-48 (sulfided) and (f) Pt/MCM-48 (after reaction).

In order to clarify the evolution of the active phase during the catalytic test, XPS analyzed were realized to the spent catalysts. The Mo $3d_{5/2}$ core level for Mo/MCM-48 and PtMo/MCM-48 catalyst show a similar trend (Fig. 5). The contribution assigned to unreduced Mo^{6+} species disappears during the catalytic test, being only noticeable the contribution assigned to MoS_2 located between 229.3 and 228.9 eV. This fact indicates that the H_2S obtained as by-product in the HDS reaction acts as sulfided agent during the catalytic test. With regards to Pt $4f_{7/2}$ core level spectra, both the contribution assigned to Pt^0 and Pt^{2+} maintains the ratio between their intensity (Fig. 4). In the same way, the surface atomic concentration of both catalysts also remains unaltered during the catalytic test, which indicates that species platinum

Table 2
Binding energies (eV) and surface atomic concentration (SAC) of core electrons in PtMo/MCM-48 catalysts in oxide precursos (O), sulfided (S) and after HDS reaction (SPR).

Catalyst	Treatment	Binding energy (eV)							
		S $2p_{3/2}$	Mo $3d_{5/2}$		Pt $4f_{7/2}$		SAC (%)		
		S^{2-}	Mo(IV)	Mo(VI)	Pt(0)	Pt(II)	S	Pt	Mo
PtMo/MCM-48	O	–	–	231.6	71.2 (81.4%)	73.2 (18.6%)	–	0.06	0.34
PtMo/MCM-48	S	162.3	228.1 (91.0%)	231.2 (9.0%)	71.5 (79.5)	73.8 (20.5%)	0.36	0.09	0.32
PtMo/MCM-48	SPR	162.3	229.3	–	71.8 (80.3)	73.3 (19.7)	0.07	0.09	0.11
Pt/MCM-48	O	–	–	–	71.2 (80.6)	73.0 (19.4)	–	0.13	–
Pt/MCM-48	S	–	–	–	71.3 (81.8)	72.7 (18.2)	–	0.11	–
Pt/MCM-48	SPR	–	–	–	71.7 (82.1)	73.3 (17.9)	–	0.09	–
Mo/MCM-48	O	–	–	232.0	–	–	–	–	0.29
Mo/MCM-48	S	161.4	228.0 (90.6)	231.9 (9.4)	–	–	0.62	–	0.45
Mo/MCM-48	SPR	162.2	228.9	–	–	–	0.10	–	0.17

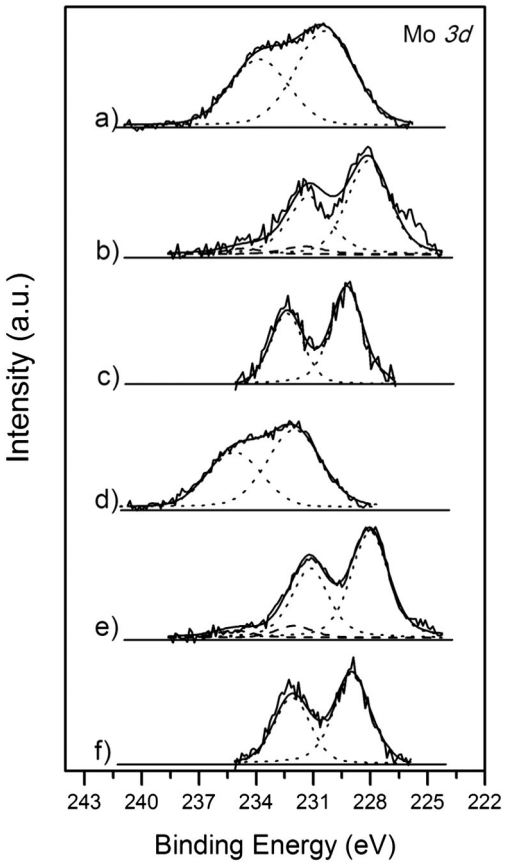

Fig. 5. Mo 3d core level spectra of PtMo/MCM-48 catalysts: (a) PtMo/MCM-48 (oxide), (b) PtMo/MCM-48 (sulfided), (c) PtMo/MCM-48 (after reaction), (d) Mo/MCM-48 (oxide), (e) Mo/MCM-48 (sulfided) and (f) Mo/MCM-48 (after reaction).

present a high tolerance to sulfur species in the HDS of DBT [30] as was suggested previously.

In accordance with the results showed in Table 4 it is possible to observe that the Mo/MCM-48 catalyst showed significant deactivation while Pt/MCM-48 and PtMo/MCM-48 not. This may be related with the sintering of MoS_2 phase present and subsequent migration of these species from the surface to the bulk. The results of XPS for the Mo/MCM-48 catalyst after the reaction showed a significant decrease in surface atomic concentration (SAC) of Mo^{4+} and S^{2-} species, and

Table 3
Conversion, yields and CHB/PB at different temperatures.

Catalyst	Temperature (°C)	Conversion (%)	Yield (%)		CHB/BP ratio
			BP	CHB	
PtMo/MCM-48	250	1.1	1.0	0.1	0.100
	275	7.9	6.7	1.1	0.164
	300	21.4	19.4	1.8	0.093
	325	47.2	39.4	4.6	0.116
	350	75.4	63.8	10.6	0.166
	375	92.3	79.2	11.9	0.150
Pt/MCM-48	250	10.9	10.5	0.2	0.019
	275	12.0	11.8	0.2	0.017
	300	20.8	20.6	0.2	0.010
	325	20.3	20.1	0.3	0.015
	350	21.6	21.5	0.3	0.014
	375	26.7	26.6	0.3	0.011
Mo/MCM-48	250	4.5	4.5	0.0	0.000
	275	5.4	5.1	0.3	0.059
	300	6.7	6.7	0.0	0.000
	325	9.3	8.9	0.4	0.045
	350	9.6	9.6	0.3	0.031
	375	17.2	17.2	0.6	0.035

Table 4
Conversion, yields and CHB/PB ratios at 350 °C at different times.

Catalyst	Time (h)	Conversion (%)	Yield (%)		CHB/BP ratio
			BP	CHB	
PtMo/MCM-48	0	83.0	68.90	12.34	0.179
	1	82.8	68.13	12.18	0.179
	2	81.0	67.68	11.4	0.168
	4	80.2	67.84	10.54	0.155
	6	80.1	67.86	10.43	0.154
	8	80.1	67.96	10.33	0.152
Pt/MCM-48	0	25.7	25.47	0.20	0.008
	1	22.2	22.04	0.16	0.007
	2	20.3	20.20	0.10	0.005
	4	18.4	18.59	0.12	0.006
	6	18.1	17.97	0.13	0.007
	8	17.9	17.77	0.12	0.007
Mo/MCM-48	0	7.1	6.95	0.15	0.022
	1	6.1	5.92	0.17	0.029
	2	4.1	3.98	0.12	0.030
	4	3.4	3.30	0.10	0.030
	6	1.6	1.56	0.05	0.032
	8	0.8	0.78	0.02	0.026

did not show bands related to Mo^{6+} species. On the other hand, after the reaction the Pt/MCM-48 catalyst showed that the SAC of platinum metallic remains practically constant and this is reflected in the catalytic test. For PtMo/MCM-48 catalyst, platinum presence inhibits the sintering effect of MoS_2 due to their promoting effect and also due to the synergistic effect that is established between the metallic platinum and MoS_2.

The results of the catalytic tests, such as the conversion levels and yield cannot be correlated with the textural characteristics of the catalysts, because the most active catalyst (PtMo/MCM-48(S)) have SSA, W_t, D_p values similar to those the catalyst that has a lower activity (Mo/MCM-48(S)), and this catalyst have much lower conversion levels than PtMo/MCM-48(S) catalyst. The higher activity of the PtMo/MCM-48(S) catalyst compared to the Pt/MCM-48 (S) and Mo/MCM-48 (S) catalysts can be correlated with the synergistic effect established between the platinum species and the MoS_2. This can be observed by the decreasing the platinum crystallite size in PtMo/MCM-48(S) in comparison with the Pt/MCM-48(S) and also through the reduced tendency to deactivation of PtMo/MCM-48(S) as compared with the catalyst Mo/MCM-48(S). Besides this, the activity of PtMo/MCM-48(S) in comparison with the catalysts Pt/MCM-48(S) and Mo/MCM-48(S) is much greater than the sum of the individual contributions that also suggests that the properties are due to the interaction established between the platinum species and MoS_2.

4. Conclusions

Hydrodesulfurization of dibenzothiophene over PtMo/MCM-48 catalysts in the sulfided form showed high conversion degrees of ca. 95%. The main obtained products were BP and CHB and the high PB/CHB ratios show that the DDS was the predominant reaction. The active phase for the reaction is composed of Pt and MoS_2 species on the MCM-48 surface. The high performance of the PtMo/MCM-48(S) catalyst can be attributed to the synergistic effect established between the species of platinum metallic and MoS_2.

Acknowledgments

The authors acknowledge CNPq — Conselho Nacional de Desenvolvimento Científico e Tecnológico (Proc.: 245544/2012-7 and 245542/2012-4) and Ministerio de Innovación y Ciencia CTQ2012-37925-C03-03/FEDER funds and Project of Excellence RNM 1565 of Junta de Andalucía.

References

[1] M. Hussain, S. Song, S. Ihm, Fuel 106 (2013) 787–792.
[2] A. Infantes-Molina, A. Romero-Pérez, E. Finocchio, G. Busca, A. Jiménez-López, E. Rodríguez-Castellón, J. Catal. 305 (2013) 101–117.
[3] R. Silva-Rodrigo, C. Calderón-Salas, J.A. Melo-Banda, J.M. Domínguez, A. Vázquez-Rodríguez, Catal. Today 98 (2004) 123–129.
[4] A. Stanislaus, A. Marafi, M.S. Rana, Catal. Today 153 (2010) 1–68.
[5] L. Cedeño, D. Hernandez, T. Klimova, J. Ramire, Appl. Catal. A Gen. 241 (2003) 39–50.
[6] M.J.B. Souza, B.A. Marinkovic, P.M. Jardim, A.S. Araujo, A.M.G. Pedrosa, R.R. Souza, Appl. Catal. A Gen. 316 (2007) 212–218.
[7] R. Navarro, B. Pawelec, J.L.G. Fierro, P.T. Vasudevan, Appl. Catal. A Gen. 148 (1996) 23–40.
[8] D. Gulkova, Y. Yoshimura, Z. Vit, Appl. Catal. B Environ. 87 (2009) 171–180.
[9] V.G. Baldovino-Medrano, S.A. Giraldo, A. Centeno, Fuel 89 (2010) 1012–1018.
[10] X. Xu, C. Song, J.M. Andresen, B.G. Miller, A.W. Scaroni, Microporous Mesoporous Mater. 62 (2003) 29–45.
[11] P.J.E. Harlick, A. Sayari, Ind. Eng. Chem. Res. 46 (2007) 446–458.
[12] M. Kruk, M. Jaroniec, R. Ryoo, J.M. Kim, Chem. Mater. 11 (1999) 2568–2572.
[13] C.T. Kresge, M.E. Leonowicz, W.J. Roth, J.C. Vartuli, J.S. Beck, Nature 359 (1992) 710–712.
[14] L. Wang, Y. Shao, J. Zhang, M. Anpo, Microporous Mesoporous Mater. 95 (2006) 17–25.
[15] M.L. Gray, Y. Soong, K.J. Champagne, H. Pennline, J.P. Baltrus, R.W. Stevens Jr., R. Khatri, S.S.C. Chuang, T. Filburn, Fuel Process. Technol. 86 (2005) 1449–1455.
[16] A.C. Sorensen, B.L. Fuller, A.G. Eklund, C.C. Landry, Chem. Mater. 16 (2004) 2157–2164.
[17] C.W. Kwong, C.Y.H. Chao, K.S. Hui, M.P. Wan, Atmos. Environ. 42 (2008) 2300–2311.
[18] A. Infantes-Molina, C. Moreno-Leon, B. Pawelec, J.L.G. Fierro, E. Rodríguez-Castellón, A. Jiménez-López, Appl. Catal. B Environ. 113–114 (2012) 87–99.
[19] J.A. Cecilia, A. Infantes-Molina, E. Rodríguez-Castellón, A. Jiménez-López, J. Catal. 263 (2009) 4–15.
[20] A. Doyle, B.K. Hodnett, Microporous Mesoporous Mater. 63 (2003) 53–57.
[21] M.J.B. Souza, A.O.S. Silva, J.M.F.B. Aquino, V.J. Fernandes Jr., A.S. Araujo, J. Therm. Anal. Calorim. 79 (2005) 493–497.
[22] T. Nguyen, M. Hilliard, G.T. Rochelle, Int. J. Greenhouse Gas Control 4 (2010) 707–715.
[23] M. Jaroniec, M. Kruk, A. Sayari, J. Phys. Chem. B 101 (1997) 583–589.
[24] Y. Chen, Y. Sun, S. Yu, C. Hsiung, J. Gan, C. Kou, Nucl. Inst. Methods Phys. Res. B 237 (2005) 296–300.
[25] A. Fritsch, P. Legare, Surf. Sci. 184 (1987) 355–360.
[26] J. Dembowski, L. Marosi, M. Essig, Surf. Sci. Spectra 2 (1993) 104–108.
[27] R. Navarro, B. Pawelec, J.L.G. Fierro, P.T. Vasudevan, J.F. Cambra, P.L. Arias, Appl. Catal. A Gen. 137 (1996) 269–286.
[28] C. Song, K.M. Reddy, Appl. Catal. A Gen. 176 (1999) 1–10.
[29] Y.W. Li, B. Delmon, J. Mol. Catal. A Chem. 127 (1997) 163–190.
[30] J. Wang, W.-Z. Li, G. Perot, J.L. Lemberton, C.-Y. Yu, C. Thomas, Y.-Z. Zhang, Stud. Surf. Sci. Catal. 112 (1997) 171–178.